

Exploring Artifact Rejection for High-pulse Rate Electrically Evoked Auditory Steady State Responses in Cochlear Implants Users

Hongmei Hu* and Stephan D. Ewert†

Medizinische Physik, Universität Oldenburg and Cluster of Excellence “Hearing4all”, Oldenburg, Germany

*E-mail: hongmei.hu@uol.de Tel: +49-44-17983380

†E-mail: stephan.ewert@uol.de Tel: +49-44-17983900

Abstract—The electrically evoked auditory steady state response (eASSR) is a potential objective measurement for cochlear implant (CI) fitting. Similar to other electroencephalography (EEG) measurements with CI users, artifacts caused by the pulsatile electric stimulation are phase locked to the stimulus and cannot be further reduced via an increasing number of repetitions. This is particularly problematic for high-pulse-rate eASSR, where the artifact temporally overlaps with a large part of the desired brain response. Here, an off-line CI artifact reduction technique, referred to as moving strobe averaging (MSA), is proposed and evaluated using highly-controlled EEG measurement data which deliberately do not contain a brain response: 1) simulated idealized data and 2) two dummy EEG recordings collected with either an electric resistor circuit to mimic scalp impedances (CI-in-a-box) or a saline solution filled tank (CI-in-a-tank) setup. The MSA algorithm supports identification of the artifact in the time domain and only requires that the artifact duration remains shorter than the inter-stimulus interval. In addition to being computationally efficient, MSA allows for removal of the stimulation artifact with minimal distortion of the desired neural response. Potential limitations of artifact rejection caused by the recording equipment itself are identified.

I. INTRODUCTION

A cochlear implant (CI) is an electrical device that helps to restore hearing to the profoundly deaf. The main principle of a CI is to directly stimulate the auditory nerve via electrodes surgically inserted into the inner ear [1]. With the increasing number of CI users, the usage of objective techniques to estimate perception thresholds and to facilitate clinical fitting of CI recipients are invaluable, especially for clinical populations who are not able to respond behaviorally to stimuli in the environment (e.g., infants). The auditory steady state response (ASSR) is one of such non-invasive objective techniques using scalp electroencephalography (EEG) recordings. It provides clinicians with important information about the auditory system and its function in various studies [2, 3]. Compared to the widely used acoustic ASSR, one outstanding issue of electrically-evoked ASSR (eASSR) with CI electrical stimulation is its inherent contamination with pulsatile artifacts from the stimulation itself. It is challenging to disentangle the electrically evoked potential from the CI artifacts because of the overlap of the eASSR and the CI stimulation artifact in the time and frequency domain [4-8]. One commonly used method for removing CI stimulation

artifacts is linear interpolation or line-out. Despite different successful applications [5, 9-11], significant distortion to the recorded signal could occur in some cases when the interpolation parameters are not carefully controlled, or the artifact and evoked potential show significant temporal overlap, especially when the analysis and decision is performed in the frequency domain. With high pulse rates, such as used in this eASSR study, widely used methods like linear interpolation for removing CI stimulation artifacts are more problematic than in low pulse rate cases as used in previous studies [10, 11].

Fig. 1 shows one example of a high-pulse-rate (HPR) EEG recording from a CI subject in a parallel study¹ processed without and with the general linear interpolation method as used in [10, 11]. The stimulation rate (f_{pps}) is 1100 pulse per second (pps). Fig. 1a shows one segment of the preprocessed signal y (blue line). Briefly, the preprocessing includes epoching, baseline correction, bandpass filtering, and averaging (please refer to [10, 11] for more details about the preprocessing). Note that the EEG recording is dominated by the sharp, high-amplitude spikes, the CI stimulation artifacts, with the desired eASSR mainly preserved in the gaps. These CI stimulation artifacts vary between subjects and depend on several factors, such as the EEG recording system setup, the position and impedance of the recording electrodes. The signal after linear interpolation of the CI stimulation artifact is shown in red. Fig. 1b and c show the single-sided amplitude spectrum below 500 Hz without and with linear interpolation, respectively.

It is conceivable that the start and end points of interpolation are critical for obtaining a faithful estimation of the desired eASSR, particularly for the HPR stimulation, with short inter-pulse intervals (IPs): The linear interpolation on the one hand reduces the CI stimulation artifacts; on the other hand, it can also introduce interpolation artifacts. This method might not completely cancel out the artifacts, but it is acceptable for low pulse rate EEG recordings that are analyzed in the time domain based on the morphology of waveforms, such as electrically evoked auditory brainstem responses (e.g., [10, 11]). However, without precise control,

¹This study was approved by the Ethics Committee of the University of Oldenburg.

abrupt changes at the start and end points of the interpolation might introduce additional unwanted frequency components, including a component at the amplitude modulation (AM) frequency (f_m) where the desired neural response is estimated. For the current extreme example, with such a high pulse rate, the recording might be completely contaminated by artifacts, and there were no artifact-free segments. Fig. 1b without linear interpolation shows a lower amplitude at the target AM component $f_m = 38$ Hz than in Fig. 1c after linear interpolation. Such a case is problematic given that eASSR analysis and decision about auditory function are based on the amplitude of that f_m component.

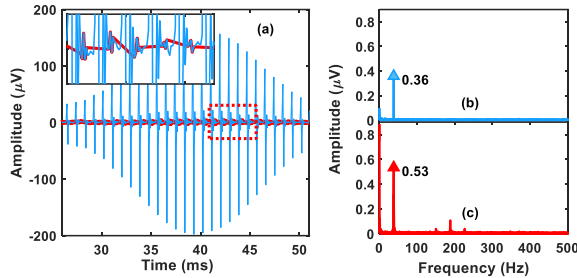


Fig. 1 EEG recordings without and with applying the general line-out method as used in [10, 11]. $f_{pps} = 1100$ pps and $f_m = 38$ Hz. (a) The blue and the red signals are the preprocessed signal without and with linear interpolation within the period of the CI stimulation artifact. (b) and (c) show the single-sided amplitude spectra below 500 Hz without and with linear interpolation, respectively.

One typical approach to separate a residual artifact at f_m from the desired neural response is the delay inherent to the neural response: Recording at several AM frequencies allows separation of artifact and neural response if it is assumed that the artifact component shows no delay and is phase-locked to the stimulation (e.g., [12]). In general, to achieve the best possible artifact rejection at f_m , the amplitude and phase of the residual artifact have to be known. To explore these two aspects, an off-line technique, named moving strobe averaging (MSA), is proposed for characterizing the amplitude and phase of the CI stimulation artifacts and for reducing the CI stimulation artifacts. With this method, the amplitude and phase of the CI artifact can be studied in isolation. The goal of this study is to assess the proposed method with simulated HPR eASSR recordings that do not contain any neural responses and to explore possible limitations of the stimulation and recording equipment that might cause or worsen the artifacts. Three types of simulated EEG signals were used: digitally generated high sampling rate sinusoidal amplitude modulated pulse trains, and EEG recordings with an implant-in-a-box (IIB) or implant-in-a-tank (IIT). The paper is organized as follows: Section II describes the proposed MSA algorithm and the experimental setup. Section III describes the validation of the MSA algorithm with different recordings. The results with and without MSA processing were compared. Finally, Section IV presents the summary and future plans. Potential limitations of artifact rejection caused by the recording equipment itself are identified.

II. METHOD

Since the AM frequency component at f_m is crucial for interpretation of eASSR data, we address i) in which case the CI stimulus itself contains an unwanted frequency component at f_m ; ii) whether temporal smearing in the EEG recording system caused by low-pass filtering affects artifact reduction, and iii) whether the artifact reduction algorithm itself can introduce or affect the frequency component at f_m . For this, theoretical (ideal) signals were generated to simulate our CI eASSR recording and analysis paradigm. The proposed MSA algorithm was first validated with these ideal signals. In order to further validate the MSA algorithm with recorded signals and to additionally characterize the CI artifacts, HPR eASSR recordings of a simulated CI dummy user were recorded via our EEG system in two highly-controlled lab setups: with either a MED-EL cochlear implant-in-a-box (IIB) or cochlear implant-in-a-tank (IIT).

A. Moving strobe averaging algorithm

The concept of the proposed MSA algorithm is to completely exclude those samples in the original recording \mathbf{y} that dominated by the CI stimulation artifact (where otherwise line-out and interpolation are applied) from the analysis and to only use the remaining (presumably clean) samples to reconstruct an artifact-reduced signal. The ‘strobe’ process in MSA means that we extract a time series of a single sample per pulse interval, separated from the next one by the duration of the IPI, thus reflecting a stimulus-driven down-sampling process. By moving the starting strobe (or sample) time point along the pulse interval, we generate a series of down-sampled recordings which contain the artifact to a different degree. The whole algorithm can be broken down into three steps:

1) *Moving strobe generation*: This reflects a moving down-sampling processing with a decimated sampling rate equal to the pulse rate. It results in a number of strobed signals $[\mathbf{z}_1, \mathbf{z}_2, \dots, \mathbf{z}_M]$, and each signal \mathbf{z}_i ($i = 1:M$) consists of a time series with one sample from each IPI. The number of strobed signals depends on the samples or moving steps M within one IPI, $M = f_s/f_{pps}$, where f_s is the sampling rate in Hz, and f_{pps} is the pulse rate in pps. In some cases it is necessary to resample \mathbf{y} to ensure the IPI (and thus M) is an integer number of samples. This decimation process assumes that the desired neural signal contains frequencies (like f_m) well below the resulting Nyquist frequency $f_{pps}/2$.

2) *CI stimulation artifact detection and reduction*: To detect and reduce the CI stimulation artifacts, the strobed signal \mathbf{z}_i is first transformed into the frequency domain \mathbf{Z}_i using a fast Fourier transform (FFT). The single-sided amplitude spectrum \mathbf{Amp}_i and the phase spectrum \mathbf{Pha}_i are obtained using Eq. (1) and (2) respectively, where N is the length of \mathbf{Z}_i in samples. The $\text{re}(\mathbf{Z}_i)$ and $\text{img}(\mathbf{Z}_i)$ are the real and imaginary parts of the complex spectrum \mathbf{Z}_i

$$\mathbf{Amp}_i = 2 \times \sqrt{(\text{re}(\mathbf{Z}_i))^2 + (\text{img}(\mathbf{Z}_i))^2} / N \quad (1)$$

$$\mathbf{Pha}_i = \text{img}(\mathbf{Z}_i) / \text{re}(\mathbf{Z}_i) \times 180 / \pi \quad (2)$$

3) *Residual strobe averaging*: The strobed signals are grouped as CI stimulation artifact dominated signal or residual signal. Based on the assumption that those strobed signals containing CI stimulation artifact samples have much larger (hundreds or thousands times) amplitudes than the neural response or EEG noise, detection and removal of the CI stimulation artifact can be achieved by comparing the amplitude at f_m , $\mathbf{Amp}_i(f_m)$, to a threshold Th . Typically, this threshold should be smaller than CI stimulation artifact but larger than the expected neural response as reported in the literature. If the amplitude $\mathbf{Amp}_i(f_m)$ of a given strobed signal \mathbf{z}_i is larger than Th , it is assumed to be CI stimulation artifact dominated, and \mathbf{z}_i is excluded from reconstruction. The remaining strobed signals are averaged for noise reduction to reconstruct the residual signal $\hat{\mathbf{y}}$. The averaging comprises lowpass filtering in decimation process. It should be noted that the residual signal could still contain artifacts, particularly when the artifact duration is larger than the IPI and no artifact-free segment exists. However, this is a general problem for HPR artifacts reduction techniques.

B. Idealized simulated recordings

1) *Stimuli*: Sinusoidally amplitude-modulated (SAM) biphasic pulse trains were generated digitally with a sampling rate of 200 kHz according to Eq. (3) to simulate idealized biphasic CI stimuli used in our eASSR paradigm.

$$s(t) = H + 0.5 * (C - H) * p(t) * [1 - \cos(2\pi * f_m * t)] * D \quad (3)$$

D is the percentage of dynamic range and f_m is the AM frequency. In this example, $f_m = 38$ Hz, $f_{pps} = 810$, $H = 147$ μ A, $C = 729$ μ A. The parameters C and H are the maximum comfortable level and hearing threshold level, respectively. In practice, these are fitting parameters for the individual CI users. Here, C and H were selected to mimic a typical CI subject from a parallel study. $p(t)$ is a biphasic pulse train (anodic pulse first), with a phase duration of 40- μ s and rate f_{pps} . Both symmetrical and asymmetrical SAM pulse trains were generated by controlling the amplitudes of anodic and cathodic pulses in $p(t)$. In an asymmetrical SAM stimulus, a ratio of 0.9 between the anodic and cathodic pulse amplitude was used. The asymmetrical example was added to demonstrate the effect of asymmetrical (charge unbalanced) biphasic pulses on the artifact at f_m . However, it should be emphasized that a non-defective CI is designed to deliver charge balanced biphasic pulses.

2) *Equipment*: In order to simulate our EEG recording system and to explore the effect of temporal smearing of the artifact by the analog low-pass (anti-aliasing) filter, the signal in Eq. (3) was first filtered with a third-order 8-kHz Butterworth low-pass filter and then down-sampled to the EEG recording sampling rate of 20 kHz.

C. Controlled lab recordings

1) *Stimuli*: The stimuli were charge-balanced biphasic SAM pulses trains (anodic pulse first) as described in Eq. (3), with 40- μ s phase duration, and 2.1- μ s interphase gap presented repeatedly via monopolar stimulation mode at 810 pps to electrode 1.

2) *Equipment*: HPR eASSRs were recorded with our EEG system using two dummy setups: 1) a self-build resistor circuit connected to the MED-EL implant-in-a-box (IIB); or 2) a MED-EL implant-in-a-tank filled with saline solution (ITT). Following this procedure, CI recordings with both CI stimulation and recording system related artifacts could be generated in a highly controlled way. The stimulation and EEG setup is shown in Fig. 2, which is part of our self-developed CI psychoacoustic and EEG experiments platform [10, 11, 13, 14]. The electrical stimuli were controlled from a stimulation PC running MATLAB via a research interface (the RIB II device, University of Innsbruck, Austria) that communicated directly with implant via a National Instruments I/O card, optical isolation interface box.

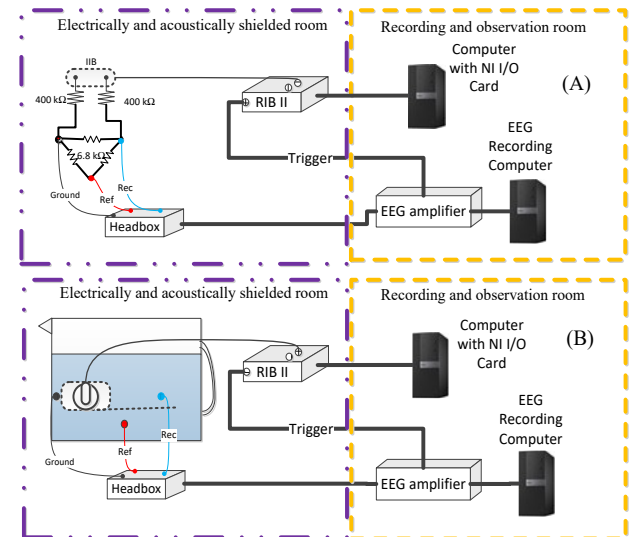


Fig. 2 (A) The setup for the EEG stimulation and EEG recording with self-build circuit and cochlear implant-in-a-box (IIB) experiment. (B) The setup for the EEG stimulation and EEG recording with a cochlear implant-in-the-tank (IIT) experiment.

Fig. 2A shows experimental setup using the the IIB-circuit. A triangle circuit with three equal resistors (6.8 k Ω) was introduced to mimic the impedance of the EEG scalp electrodes of real subjects. The two 400-k Ω resistors connected to the CI electrode and ground of the IIB were used to protect the EEG amplifier from over loading. The three nodes of the equal-resistance triangle circuit were connected to three EEG recording electrodes (reference, ground and recording) as shown in Fig. 2A. For the IIT experiment, the stimulation and EEG setup is similar to Fig. 2A and is shown in Fig. 2B. Here, a MED-EL Synchrony implant was placed together with three EEG recording electrodes (reference, ground and recording) in a head-sized container filled with 0.2% saline solution. The EEG recording electrode was placed to the contralateral side of the CI inside the same tank. For both setups, EEG data were differentially recorded from 3-channel Ag/AgCl electrodes (Fig. 2). The scalp electrodes were connected to the three monopolar input connectors of a SynAmps RT amplifier system (Neuroscan). The IIB-circuit or IIT setup was placed in an electrically shielded sound-attenuating booth. The artifact rejection was turned off, the sweeps were filtered by an analog antialiasing-low-pass filter

with a corner frequency of 8 kHz, digitized with 20 kHz sampling rate via a 24 bit A/D convertor, and stored to hard disk. The recording software was CURRY 7 (Neuroscan). Ten sweeps were repeated for each condition. Each recording sweep consisted of 18 blocks, each block lasting 1 s.

III. RESULTS

A. Idealized simulated HPR AM recordings

Fig. 3 shows the asymmetrical (column 1, orange), symmetrical (column 2, blue) SAM biphasic pulse trains, and the symmetrical pulse train after low-pass filtering (column 3, red) and following down-sampling (column 4, black). The bottom panel of Fig. 3 shows the single-sided amplitude spectrum obtained according to Eq. (1), below 900 Hz. As expected from theory, there is no frequency component at f_m for all symmetrical stimuli (charge balanced pulses), but for the asymmetrical stimulus. Although CI stimulation is intended to be charge-balanced (symmetrical), this case demonstrates the (de-modulating) effect of an asymmetric non-linearity at any stage of the processing. It should be noted that the frequency component at f_m in the artifact is critical for the eASSR measurement because of the spectro-temporal overlap of the desired neural response and the artifact.

The magnified small inserts in Fig. 3 highlight that the low-pass filtering (column 3, red) introduced some noticeable tail oscillations (filter ringing) and a widening of the recorded pulses (simulated CI stimulation artifacts) near the baseline amplitude (0 in this example). In addition, the down-sampling (column 4, green) introduced additional oscillations and widening. Consequently, these operations temporally smeared the stimulation artifacts and reduced the artifact-free samples within each IPI, which can affect artifact rejection, especially for HPR CI artifact reduction algorithms. However these (linear) operations cannot introduce a frequency component at f_m .

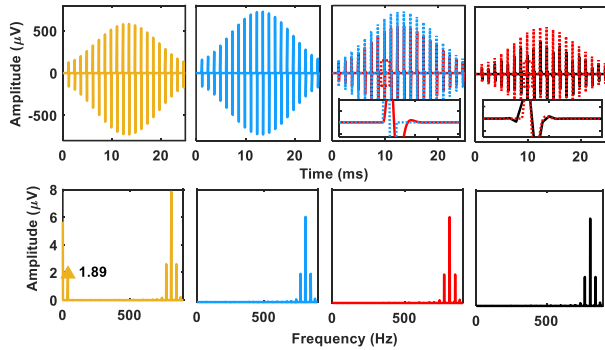


Fig. 3 The asymmetrical (column1, orange), and the symmetrical (biphasic; column 2, blue) SAM signals used for the EEG stimulation. The SAM symmetrical biphasic pulse trains after low-pass filtering (column 3, red) and down-sampling (column 4, black).

Fig. 4 shows an example of applying the MSA algorithm to the simulated EEG signal (column 4, Fig. 3, after low-pass filtering and downsampling). Fig. 4a shows one modulation cycle of the signal. The small insert is a magnification of the area within the dotted red rectangular box. The asterisk, solid and open circles are three example strobed signals within time

range of [0 26] ms at the following (moving) strobe steps, i , within the IPI: $i = 1$ (red open circles at the positive peak), $i = 7$ (black solid circles), $i = 9$ (green asterisks at the negative peak). Fig. 4b shows the resulting strobed time signals for all strobe steps from $i = 1$ to $i = 25$; the corresponding steps are marked with the corresponding number. Fig. 4c shows a waterfall plot of all strobed time signals. Fig. 4d is the single-sided amplitude spectrum (blue) and the corresponding phase spectrum (green) at frequency f_m for different strobes.

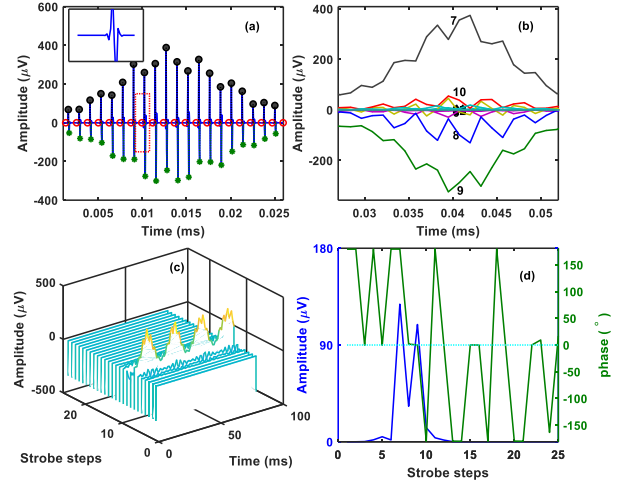


Fig. 4 Example of applying the MSA algorithm on the ideal symmetrical signal. fpps = 810, $f_m = 38$, fs = 20 kHz. (a) Simulated EEG signal in one AM cycle. (b) Strobed time signal with strobe steps of 1-25. (c) Waterfall plot of the strobed time signal, with strobe steps of 1-25. (d) The single-sided amplitude spectrum (blue) and the corresponding phase (green) of component f_m for each strobe (1-25).

The phases at frequency f_m of all the strobes, shown in Fig. 4d (green), are either $\pm 180^\circ$ or 0° , corresponding to the polarity of the artifact in the strobe (negative peaks correspond to 0° phase of the envelope at f_m). The maximum amplitudes occur within steps 5-12, which are the strobes dominated by the CI biphasic stimulation artifact. The strobes outside of this range can be treated as residual signals that might be suited to estimate the neural (brain) response in a real recording. In order to show how to remove the strobes dominated by the CI stimulation artifacts and how to reconstruct the residual signal from the remaining strobes, the strobes between steps 19-25 were used in the construction. The same strobes were used for a comparison with the IIB and IIT setups.

Fig. 5a and f (green) shows the reconstructed signal from the average of the strobed signals of $[z_{19}, z_{20}, \dots, z_{25}]$. The amplitude (note the 1000 times smaller scale in the y-axis) at $f_m = 38$ Hz is 0.53 nV, which is hundreds of times smaller than a typical eASSR response (about 0.05-0.6 μ V, e.g., [15]). This demonstrates that MSA is suited to successfully identify and reject the stimulation artifact under ideal conditions.

B. Controlled lab recordings

Fig. 5 shows the amplitude of the recorded data after preprocessing for IIB-circuit (column 2, orange) and IIT

(column 4, blue) in the time (b, d) and frequency (g, i) domains, respectively. In contrast to the previous ideal case, both recordings show a response at the modulation frequency ($f_m=38$ Hz). This implies there might be non-linearities or asymmetric features in the system. Note that the IIB signal is more than 10 times larger than the IIT signal. Column 3 and 5 of Fig. 5 show the corresponding MSA processed signals.

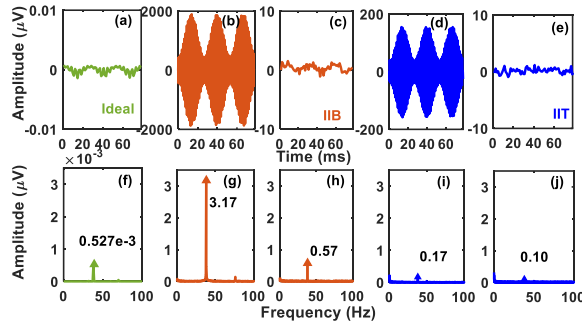


Fig. 5 The amplitude of the recording data after preprocessing (b, g, IIB-circuit; d, i, IIT) and after MSA (a, f, ideal symmetric signal; c, h, IIB-circuit; e, j, IIT) in the time (a - e) and frequency (f - j) domains.

In order to identify and remove CI stimulation dominated strobos, for demonstration purposes, here solely the strobe amplitudes without considering the phase information shown in Fig. 6A and B (panel d, blue) were used. The rejection threshold Th was set to $1 \mu V$, which means all the strobos with amplitudes larger than $1 \mu V$ were assumed to be dominated by CI stimulation artifacts. In real applications, the selection or the estimation of the strobe rejection threshold is important for identifying the strobos dominated by the CI stimulation artifacts. More advanced methods, such as machine learning (e.g., deep neural networks) could be useful for estimating the Th in the future. The artifact-reduced signals shown in Fig. 5 (c, h, IIB-circuit; e, j, IIT) were reconstructed only with the strobos between step 19 and step 25. The residual spectrum amplitude of the IIB-circuit recording (Fig. 5c, h) at f_m (38 Hz) is 1000 times larger than that in the ideal signal (Fig. 5a, f) and nearly 6 times larger than the IIT recording (Fig. 5e, j). The difference between the residual amplitude of IIB-circuit and IIT recordings are mainly caused by the differences of effective impedance between these two experimental setups and the amplitude difference of the preprocessed signals (1897 and $155 \mu V$ peak, respectively). Taking these amplitude differences into account and assuming linearity, the residual in the IIB signal is actually smaller than in IIT: $0.57/1897 \times 155 \mu V = 0.05 \mu V$. This suggests that non-linearities are larger in the tank than in the resistor circuit.

Fig. 6 shows how these MSA processed signals were obtained for the IIB-circuit (A) and IIT recordings (B): $f_{pps}=810$, $f_m = 38$ Hz, $f_s = 20$ kHz. During moving strobos generation, in this example, the 7th and 9th strobos were the samples at the positive peak and the negative peak of the artifact, respectively. Comparing the single-sided amplitude spectrum in Fig. 4d and Fig. 6d, the patterns of the amplitude spectrum are very similar among these three recording types except for the absolute values. The artifact peaks are all

within steps 5 to 12. One important difference to the ideal case in Fig. 4d is that the phases of the strobos between [19 25] are neither exactly zero nor $\pm 180^\circ$ in Fig. 6A and B (panel d). Such distortions affecting the residual artifact phase at f_m might be relevant if phase is used to separate neural response and artifact (e.g., [12]).

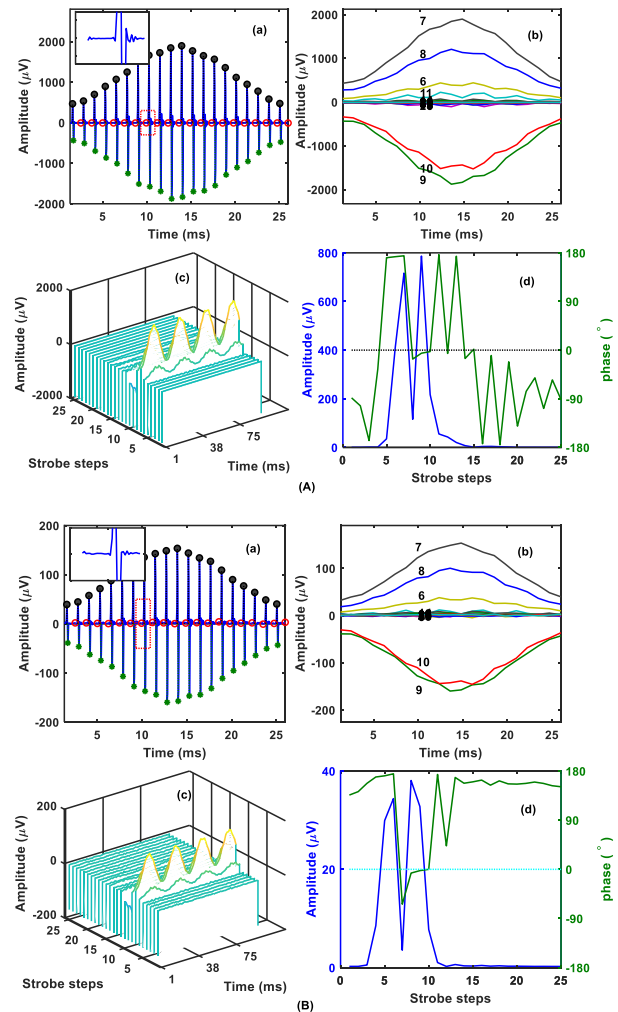


Fig. 6 MSA algorithm applied to IIB-circuit (A) and IIT recordings (B). (a) Preprocessed EEG signal in one AM cycle. The small insert magnifies the dotted red rectangular box. The asterisk, solid, and open circles are three example strobos within the time range of [0 26] ms at the following steps: 1st (open circles at the positive peak), 7th (solid circles), 9th (asterisks at the negative peak). (b) Strobed time signal with strobe steps of 1-25. (c) Waterfall plot of the strobed time signal, with strobe steps of 1-25. (d) The single-sided amplitude spectrum (blue) and the corresponding phase (green) of component f_m for each strobe (1-25).

The residual signal of the ideal simulated symmetrical recording after MSA has near zero amplitude at f_m , and the residual strobos had either zero or $\pm 180^\circ$ phase. However, both dummy recordings (IIB and IIT) show more eASSR-like residual signals: less than $1 \mu V$ (~hundreds of nV) amplitude at the modulation frequency and not exactly zero or $\pm 180^\circ$ phase. Theoretically, the phase information could be used in assisting the artifact detection, however, the non-zero (or non

$\pm 180^\circ$) phase present in both IIB-circuit and IIT recordings implies that caution has to be taken.

Taken together, it is observed that: 1) MSA dramatically reduces the CI stimulation artifacts in the time domain. 2) All signals, without and with MSA algorithm show a frequency component at f_m . 3) The frequency component at f_m was smaller than $1 \mu\text{V}$ (except for the IIB-circuit) even without artifact reduction. 4) The proposed MSA algorithm reduces the residual artifact at f_m . It needs to be emphasized, that the data used here for demonstration are dummy recordings which do not contain any neural response at f_m . Nevertheless, unlike in the ideal case, a small component at f_m occurs in the recordings. The current results thus suggest that caution should be taken in interpreting eASSR results containing a small f_m component, particularly given that in the real recordings phase distortions of residual component at f_m might occur. Thus in practice, additional measures to reduce the residual artifact like alternating polarity stimulation (e.g., [10, 11]) are advisable.

One further advantage of the proposed MSA algorithm is the easily assessable identification and characterization of the artifact in the strobed waterfall plot and the amplitude/phase plot. For the application of MSA algorithm, additional tests such as, e.g., subthreshold (below the perceptual level threshold) recording and loudness growth functions, might be helpful in real CI users.

IV. SUMMARY AND CONCLUSIONS

A simple CI artifact reduction method named MSA has been proposed and tested with different setups: high pulse rate eASSR simulation and dummy recordings from a cochlear implant-in-a-box circuit and a cochlear implant-in-a-tank setup. Overall, the study shows:

1) The proposed MSA algorithm can remove the CI stimulation artifact with minimal distortion of the residual signal by skipping the strobos clearly dominated by stimulation artifact. This technique only requires that the artifact strobos are identifiable in the suggested graphical depiction of the analysis and the artifact duration is shorter than both the inter-stimulus interval and the time course of the desired neural response. This limitation also holds for other techniques.

2) The residual artifact visible in dummy recordings suggests that attention should be paid when interpreting the eASSR component at the AM frequency. Such artifact might be contained in eASSR recordings of CI subjects. Information can be gathered from dummy recordings of the suggested IIB or IIT setup together with sub-threshold eASSR recordings from each CI user. Based on these additional recordings, the residual artifact after MSA processing can be judged negligible or not.

V. ACKNOWLEDGMENTS

This work was partially funded by MED-EL, DFG (352015383 - SFB 1330 A2), MRC Grant (MR/S2002537/1). The authors are grateful to Stefan Strahl for RIB II support

and initial discussions and to Mathias Dietz and Konrad Schwarz for comments on an earlier version of the manuscript.

VI. REFERENCES

- [1] B. S. Wilson and M. F. Dorman, "The Surprising Performance of Present-Day Cochlear Implants," *Biomedical Engineering, IEEE Transactions on*, vol. 54, pp. 969-972, 2007.
- [2] T. W. Picton, M. S. John, A. Dimitrijevic, and D. Purcell, "Human auditory steady-state responses," *Int J Audiol*, vol. 42, pp. 177-219, Jun 2003.
- [3] P. Korczak, J. Smart, R. Delgado, T. M. Strobel, and C. Bradford, "Auditory steady-state responses," *Journal of the American Academy of Audiology*, vol. 23, pp. 146-170, 2012.
- [4] F.-C. Jeng, P. J. Abbas, C. J. Brown, C. A. Miller, K. V. Nourski, and B. K. Robinson, "Electrically evoked auditory steady-state responses in Guinea pigs," *Audiology & neuro-otology*, vol. 12, pp. 101-12, 2007.
- [5] M. Hofmann and J. Wouters, "Electrically evoked auditory steady state responses in cochlear implant users," *Journal of the Association for Research in Otolaryngology : JARO*, vol. 11, pp. 267-82, 2010.
- [6] M. Menard, S. Gallego, E. Truy, C. Berger-Vachon, J. D. Durrant, and L. Collet, "Auditory steady-state response evaluation of auditory thresholds in cochlear implant patients," *Int J Audiol*, vol. 43 Suppl 1, pp. S39-43, Dec 2004.
- [7] C.-H. Yang, H.-C. Chen, and C.-F. Hwang, "The prediction of hearing thresholds with auditory steady-state responses for cochlear implanted children," *International Journal of Pediatric Otorhinolaryngology*, vol. 72, pp. 609-617, 2008.
- [8] M. Hofmann and J. Wouters, "Improved electrically evoked auditory steady-state response thresholds in humans," *Journal of the Association for Research in Otolaryngology : JARO*, vol. 13, pp. 573-89, 2012.
- [9] L. F. Heffer and J. B. Fallon, "A Novel Stimulus Artifact Removal Technique for High-Rate Electrical Stimulation," *Journal of Neuroscience Methods*, vol. 170, pp. 277-284, 2008.
- [10] H. Hu and M. Dietz, "Comparison of interaural electrode pairing methods for bilateral cochlear implants," *Trends in Hearing*, vol. 19, December 1, 2015 2015.
- [11] H. Hu, B. Kollmeier, and M. Dietz, "Reduction of stimulation coherent artifacts in electrically evoked auditory brainstem responses," *Biomedical Signal Processing and Control*, vol. 21, pp. 74-81, 2015.
- [12] R. Gransier, H. Deprez, M. Hofmann, M. Moonen, A. van Wieringen, and J. Wouters, "Auditory steady-state responses in cochlear implant users: Effect of modulation frequency and stimulation artifacts," *Hearing Research*, vol. 335, pp. 149-160, 2016.
- [13] S. D. Ewert, "AFC - a modular framework for running psychoacoustic experiments and computational perception models," presented at the in Proceedings of the International Conference on Acoustics (AIA-DAGA 2013), 2013.
- [14] H. Hu, S. Ewert, T. Campbell, B. Kollmeier, and M. Dietz, "An Interaural Electrode Pairing Clinical Research System for Bilateral Cochlear Implants," presented at the the 2nd IEEE China Summit and International Conference on Signal and Information Processing (ChinaSIP' 14), Xi'an, China, 2014.
- [15] M. Van Eeckhoutte, D. Spirrov, J. Wouters, and T. Francart, "Objective Binaural Loudness Balancing Based on 40-Hz Auditory Steady-State Responses. Part II: Asymmetric and Bimodal Hearing," *Trends in hearing*, vol. 22, pp. 2331216518805363-2331216518805363, Jan-Dec 2018.